Bioactive Materials 21 (2023) 253–266

Contents lists available at ScienceDirect

Bioactive Materials

journal homepage: www.keaipublishing.com/en/journals/bioactive-materials

# Living symbiotic bacteria-involved skin dressing to combat indigenous pathogens for microbiome-based biotherapy toward atopic dermatitis

Xinhua Liu [a], Youteng Qin [a], Liyun Dong [b], Ziyi Han [a], Tianning Liu [a], Ying Tang [c], Yun Yu [a], Jingjie Ye [a], Juan Tao [b], Xuan Zeng [a,**], Jun Feng [a,*], Xian-Zheng Zhang [a,***]

[a] Key Laboratory of Biomedical Polymers of Ministry of Education & Department of Chemistry, Wuhan University, Wuhan, 430072, PR China
[b] Department of Dermatology, Union Hospital, Tongji Medical College, Huazhong University of Science and Technology, Wuhan, 430074, PR China
[c] State Key Laboratory Breeding Base of Basic Science of Stomatology (Hubei-MOST) & Key Laboratory of Oral Biomedicine of Ministry of Education (KLOBM), School and Hospital of Stomatology, Wuhan University, Wuhan, 430079, PR China

ARTICLE INFO

*Keywords:*
Atopic dermatitis
Skin symbiotic bacteria
Skin dressing
Indigenous pathogens
Microbiome-based biotherapy

ABSTRACT

Many skin diseases, such as atopic dermatitis (AD), are featured with the dysbiosis of skin microbiota. The clinically recommended options for AD treatments suffer from poor outcomes and high side-effects, leading to severe quality-of-life impairment. To deal with this long-term challenge, we develop a living bacterial formulation (Hy@Rm) that integrates skin symbiotic bacteria of *Roseomonas mucosa* with poly(vinyl pyrrolidone), poly (vinyl alcohol) and sodium alginate into a skin dressing by virtue of the $Ca^{2+}$-mediated cross-linking and the freezing-thawing (F-T) cycle method. Hy@Rm dressing creates a favorable condition to not only serve as extrinsic culture harbors but also as nutrient suppliers to support *R. mucosa* survival in the harsh microenvironment of AD sites to defeat *S. aureus,* which predominantly colonizes AD skins as an indigenous pathogen, mainly through the secretion of sphingolipids metabolites by *R. mucosa* like a therapeutics bio-factory. Meanwhile, this elaborately designed skin dressing could accelerate wound healing, normalize aberrant skin characters, recover skin barrier functions, alleviate AD-associated immune/inflammation responses, functioning like a combinational therapy. This study offers a promising means for the topical bacteria transplant to realize effective microbe biotherapy toward the skin diseases feature with microbe milieu disorders, including but not limited to AD disease.

## 1. Introduction

Atopic dermatitis (AD), also named eczema, is a highly widespread inflammatory skin disease that affects 20% of children and 5% of adults in developed countries [1]. As well known for its severe quality-of-life impairment, AD disease commonly comes with the chronic, relapsing, intensely itchy and inflamed skin lesions, skin infections, tissue injuries and even systemic allergic immune responses [2–4]. Recent studies manifest that many skin diseases including AD, are featured with the dysbiosis of skin microbiota. In the AD-localized skins, microbial diversity usually drops sharply and finally pathogenic *S. aureus* takes a leading position together with *Candida* and *Trichophyton* and plays a key role in AD progression [5–7]. One unwanted outcome is the deficiency of the sphingolipids and antimicrobial peptides in the diseased skins while these two constitute epidermal permeability barrier (EPB) with a broad-spectrum defense against multiple pathogens [5–7]. Due to the complex mechanism implicated in AD disease originating from the dysbiosis of skin microbiota, patients with AD are clinically recommended to adopt combinational therapies mostly based on antibacterial treatment, anti-inflammatory therapy like glucocorticoid medication, and immune suppression [8]. However, clinical AD therapies still suffer from poor performances. Moreover, administration of antibiotics and hormone drugs with high frequency leads to the destruction of locally normal microbiota and the drugs resistance [9–11]. New strategies are needed to deal with this long-term challenge.

Microbiome-based biotherapies have attracted increasing attention

Peer review under responsibility of KeAi Communications Co., Ltd.
* Corresponding author.
** Corresponding author.
*** Corresponding author.
*E-mail addresses:* xuanzeng@whu.edu.cn (X. Zeng), fengjun@whu.edu.cn (J. Feng), xz-zhang@whu.edu.cn (X.-Z. Zhang).

https://doi.org/10.1016/j.bioactmat.2022.08.019
Received 27 May 2022; Received in revised form 8 August 2022; Accepted 23 August 2022

in treating many diseases. Living bacteria, particularly symbiotic bacteria and probiotics, have been extensively employed for add-on therapy [12,13]. For example, several commensal skin bacteria (e.g., *R. mucosa*) were reported to secrete peptides or sphingolipids to prevent the *S. aureus* mediated disruption of epidermal barrier and skin inflammation [2,4,14]. Owing to the quorum sensing among bacteria, certain probiotics may also exert a positive impact on skin diseases curation [15]. *S. epidermidis* and *S. hominis* strains were applied to suppress *S. aureus* colonization for AD patients [16,17]. Besides, bacterial lysates, bacteriophage-derived enzymes, beneficial commensals, have been used to restore healthy skin microenvironment, reduce pathogenic drivers of AD, and recover commensals in AD patients [18–20]. Although these pioneering researches adumbrate the potentials of microbial therapy, microbes alone fail to produce sufficient therapeutic activity in most cases because of their difficult colonization in the diseased sites that have been occupied by the disease-associated pathogens [21]. As the typical example, skin bacterial transplant (SBT), an intriguing treatment modality for the restoration of a healthy skin microbiome in AD patients, is still required to optimize the formulation of bacterial species, which plays a crucial role in microbial transplantation [19]. In fact, allergy and inflammatory diseases, such as AD and psoriasis, are identified with the deficiency of gram-negative bacteria owing to the disease-determining competitive superiority of certain pathogenic microbes [22]. Consequently, despite the transplanted microbes are administrated in a high dosage, therapeutic efficacy cannot last long enough [23]. Microbiome-based biotherapy has thus to cooperate with other therapy approaches for combinational therapies, and therein the contribution of transplanted microbes is still far from satisfactory. At this point, artificially creating a benign condition in the AD-localized skins to support the survival of therapeutic microbes is of great importance to the microbiome-based biotherapy toward AD disease.

Currently, living cells engineered by biomaterials have attracted rapidly increasing interests in treating various diseases, which are sometimes referred to as material-assisted micro-organisms (MAMO) [24–27]. The fusion of materials with cells allows chances to tailor cellular biofunctions in diverse fashions. Polymeric scaffolds, could accommodate cells for proliferation or differentiation in a non-evolutionary way at the site of interest [28]. Inspired by MAMO concept, we intend to develop an AD-specific living bacterial formulation for the boosted therapeutic activity to defeat AD-colonized indigenous pathogens. If established, this medication may be a revolutionary alternative to traditional AD therapy modalities. To our knowledge, the studies regarding this idea have been rarely reported.

Specifically, we designed a *R. mucosa* involved skin dressing that could enable long-term colonization of *R. mucosa* in AD-localized skins with continuous production of sphingolipids like a therapeutic biofactory to inhibit the proliferation of pathogenic *S. aureus*, and normalize the aberrant barrier functions of skins (Scheme 1). By means of the $Ca^{2+}$-mediated physical cross-linking and the freezing-thawing cycle method, *R. mucosa* was arranged to integrate with poly(vinyl pyrrolidone) (PVP), poly(vinyl alcohol) (PVA) and sodium alginate (SA) into a bacterial-involved skin dressing hydrogel (Hy@Rm). Hy@Rm dressing is allowed to not only serve as extrinsic culture harbors but also provide polymeric nutrients to support *R. mucosa* proliferation in the harsh microenvironment of AD sites, which fails by conventional methods due to the competitive superiority of pathogenic microbes over the transplanted bacteria in the AD-localized skins. What's more, Hy@Rm dressing is expected to relieve inflammation, boost epithelial

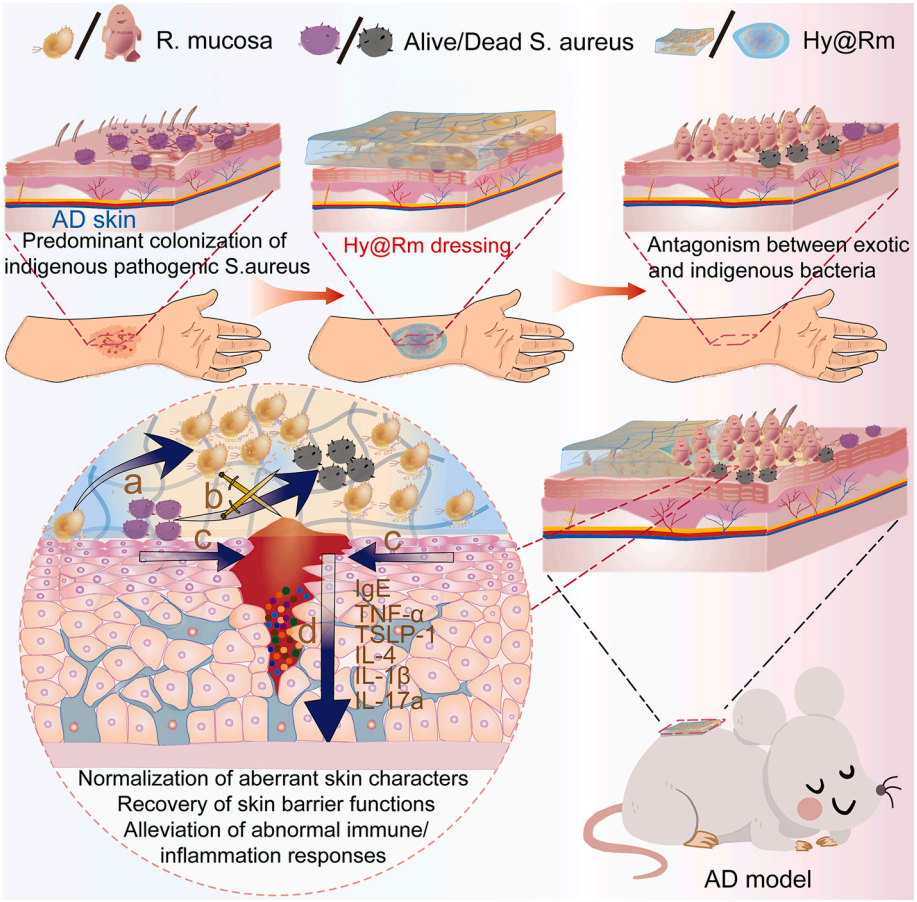


**Scheme 1.** Schematic illustration of AD mouse treated with Hy@Rm dressings. a) This dressing agent acts as culture harbor and nutrient supplier to support *R. mucosa* survival. b) *R. mucosa* secrets sphingolipids to kill *S. aureus* in AD-localized sites. c) Hy@Rm dressing facilitates epithelial migration and proliferation to benefit epithelial regeneration and wound healing. d) Hy@Rm dressing alleviates abnormal inflammatory/immune responses.

migration and proliferation, accelerate epithelial regeneration and wound healing. In this way, the treatment with Hy@Rm dressing functions actually like a combinational therapy. This study offers a promising means for the topical bacteria transplant to realize effective microbiome-based biotherapy toward the skin diseases feature with microbe milieu disorders, including but not limited to AD disease.

## 2. Materials and methods

### 2.1. Materials

2,4-dinitrochlorobenzene (DNCB) was purchased from Aladdin, PVP-K90 (Mw = 360000 g/mol) and PVA (Mw = 31000 g/mol, degree of alcoholysis, 87–89%) were obtained from Heowns. Sodium alginate (SA, Mw = 130000 g/mol) was purchased from Sinopharm Chemical Reagent (Co., Ltd). Reasoner's 2A (R2A) broth and Luria-Broth (LB) medium were obtained from Guangdong Huankai Microbial SCI&Tech Co., Ltd, agar was gained from BioLegend (USA). D-erythro-spingosine-1-phospate (DESP, Mw = 379.12 g/mol, CAS: 26993-30-6), Cyanine 5 NHS ester (Cy5-NHS), Cyanine 7 amine (Cy7-$NH_2$) were obtained from Aladdin. Vancomycin and amphotericin B were purchased from Aladdin (shanghai, China), high-glucose Dulbecco's modified Eagle's medium (DMEM), Minimum Essential Medium (MEM), penicillin–streptomycin, fetal bovine serum (FBS), Roswell Park Memorial Institute (RMPI) 1640 medium, and trypsin were provided by Invitrogen (USA). 3-[4,5-Dimethylthiazol-2-yl]-2,5-diphenyltetrazoliumbromide (MTT) was supplied by Beyotime Biotechnology Co. Ltd. Transwells were obtained from Corning Coatar. Carbonized diimide (EDC) and N-hydroxysuccinimide (NHS) were purchased from Sinopharm Chemical Reagent (Co., Ltd) without further purified. *S. aureus* (ATCC 6538) and *E. coli* (ATCC 23716) were purchased from China General Microbiological Culture Collection Center (Beijing, China).

#### 2.1.1. Characterization

Scanning electron microscopy (SEM) images were recorded by a scanning electron microscope (Zeiss Sigma). In vivo imaging was conducted by the Spectrum Pre-clinical In Vivo Imaging System (IVIS, PekinEmer). The cell viability was measured by the microplate reader (Bio-Rad, Model550, USA). Blood routine analysis was examined by Auto Hematology Analyzer (MC-6200VET) and blood biochemistry analysis was conducted by biochemical auto analyzer (MNCHIP, Tianjin, China). Trans-epidermal water loss (TWEL) was measured by TEWL tewameter (TM300) (Cologne, Germany). Skin hydration, and skin elasticity were evaluated by Imate Skin Moisture Tester (M − 6602). Scratch wound-healing assay was carried out by fluorescence inverted microscope (Olympus IX73P2F). Mass spectrometry was performed by Liquid chromatography coupled with tandem mass spectrometry (LC-MS/MS) (Agilent 1290 uplc and Agilent qtof 6550). Confocal microscopy images were recorded on a confocal laser scanning microscope (CLSM) (Nikon C1-si TE2000). Enzyme-linked immunosorbent assay kits were provided by Multi Science.

### 2.2. R. mucosa collection and identification

#### 2.2.1. R. mucosa isolation and collection

*R. mucosa* strains were obtained from the healthy volunteers. Their skins at the volar forearm were rubbed vigorously with two germfree swabs moistened by 200 μL of sterile phosphate buffer solution (PBS) for 20–30 s (n = 7). One swab was put into a conical tube with 5 mL of sterile R2A broth containing vancomycin (300 μg/mL) and amphotericin B (5 μg/mL) to suppress growth of Gram-positive bacteria and fungi. These tubes were placed into the shaking incubator at 30 °C with 180 rpm/min for 10 days. Then 100 μL liquid was taken out from each tube and plated on R2A agar plate. At the predetermined intervals, the bacteria were assessed to exclude the production of other species. *R. mucosa* strains were identified based on the morphological observation (Fig. S1) over unique colony, and the species identification experiment according to National Center for Biotechnology Information (NCBI) database.

#### 2.2.2. Polymerase chain reaction (PCR) assay for strain characterization

Primers 27F (5′-AGAGTTTGATCCTGGCTCAG-3′) and primers 1492R (5′- GGTTACCTTGTTACGACTT-3′) were used to amplify the primer sequence. The experiment procedure was referenced to the previous report [29]. Through PCR assay, the whole genomic sequence of *R. mucosa* was verified according to NCBI database.

### 2.3. Gel formation and characterization analysis

PVP/PVA/SA blended hydrogels (Hys) were fabricated via a $Ca^{2+}$-mediated physical cross-linking method and the freezing-thawing (F-T) cycle technique [30]. Briefly, 10% (w/v) PVA, 10% (w/v) PVP, and 2% (w/v) SA solution were prepared in deionized water at 60 °C. Then, polymeric solutions were mixed at different volume ratios of PVP/PVA/SA including 5/5/1, 5/5/2, 5/5/3, 5/5/4, 5/5/5. The mixture solutions were subjected to vortexing for half an hour, followed by freezing at −20 °C for 20 h and thawing at room temperature for 4 h, with three consecutive cycles. After three F-T cycles, 1 mL of ice-cold calcium phosphate solution (pH = 4.8) containing 12.5 mM of $CaCl_2$ was mixed with the solutions of PVP/PVA/SA and further shaken for 10 min to obtain PVP/PVA/SA/$Ca^{2+}$ hydrogel. Regardless of the composition of PVP/PVA/SA solutions, the molar feeding ratio of SA monomer versus calcium ion was fixed at 2:1. Hy@Rm dressing was prepared in a similar procedure. Specifically, *R. mucosa* was cultured in 30 mL of LB medium at 37 °C for 2 days under shaking at 180 rpm. The sub-cultured *R. mucosa* were collected by centrifugation (6000 rpm, 3 min) and washed with PBS thrice. *R. mucosa* strains were resuspended in 1 mL of ice-cold calcium phosphate solution containing 12.5 mM of $CaCl_2$ and the mixture was next vortexed for 5 min. The solution was mixed with the solutions of PVP/PVA/SA with a fixed molar feeding ratio of SA monomer versus calcium ion at 2:1 and then shaken for 10 min to obtain Hy@Rm dressing. Hy@Rm dressing was stored in sealed containers at 4 °C for further use.

#### 2.3.1. Bacterial viability in Hy@Rm dressing

Hy@Rm dressing ($5 \times 10^8$ CFU of *R. mucosa* in 200 μL of hydrogel) and free *R. mucosa* ($5 \times 10^8$ CFU in 200 μL of PBS) were incubated at 37 °C for 0, 12, 24, 36, 48, 72 h, respectively (n = 3). Then, Hy@Rm dressing and free *R. mucosa* were homogenized, diluted to different concentration in PBS, and plated on R2A plates. The bacterial viability was measured by the plate-count method. To study viability of *R. mucosa* in the Hy@Rm or in PBS at different storage temperatures, Hy@Rm and free *R. mucosa* were stored at room temp, 4 °C, or −20 °C for different time before viability tests.

### 2.4. Sphingolipids extraction and detection

50 mL of $5 \times 10^8$ CFU $mL^{-1}$ *R. mucosa* were cultured in a R2A broth for 2 days. *R. mucosa* strains were isolated by centrifuging at 6000 rpm for 3 min, the supernatant was extracted twice by the mixture containing chloroform, methanol, and water at the volume ratios of 1: 2: 0.8 and 2: 2: 1.8, respectively. The upper phase contained the nonlipid substances, while most lipids remained in the lower. The lipid substances were evaporated, dried in vacuum at 40 °C for 2 days, and then quantified by LC-MS/MS according to the reported method [31].

### 2.5. Antibacterial assays of R. mucosa and Hy@Rm dressing

#### 2.5.1. In vitro S. aureus and E. coli inhibition assays of medium of R. mucosa

*S. aureus* or *E. coli* strains were cultured in 15 mL of LB medium overnight. $10^5$ CFU of *R. mucosa* strains were aerobically cultured in 30 mL of LB medium for 48 h. The *R. mucosa* containing medium was

centrifuged and the supernatant was filtered (pore size = 0.22 μm), and diluted by fresh LB medium to different concentrations ready for usages. As the control, the supernatant was replaced by PBS for comparison.

$10^5$ CFU of *S. aureus* or *E. coli* strains were cultured in 1 mL of the as-obtained *R. mucosa*-containing mediums for 24 h at 37 °C under stirring. After dilutions and plating, bacterial colonies were counted in the next day. Viability of *S. aureus* or *E. coli* was calculated via dividing the colony number of *S. aureus* or *E. coli* strain in the presence of *R. mucosa* by the colony number incubated in the PBS control.

#### 2.5.2. In vitro bacterial antagonism of Hy@Rm dressing against pathogenic bacteria

Hy@Rm dressing (200 μL, $1 \times 10^7$ CFU of *R. mucosa*), 200 μL bare *R. mucosa* ($1 \times 10^7$ CFU), 200 μL of PBS (as negative control) were added into 4 mL of fresh LB medium, respectively. Then, the equal amount of *S. aureus* or *E. coli* was introduced. After incubation for 24 or 48 h at 37 °C under stirring, the culture medium was diluted, and plated evenly on specifically selective plates of *S. aureus* and *E. coli*. Bacterial colonies were counted in the next day (n = 3).

#### 2.5.3. Bacterial disk diffusion test

The antibacterial activity of *R. mucosa* extract was tested against *S. aureus*. Paper disks (6 mm diameter) were immersed in *R. mucosa* extract (8 mg/ml), the hydrogel, solution of DESP (0.17 mg/mL), sterile PBS (as negative control) for 30 min, respectively. *S. aureus* strains (100 μL,$10^5$ CFU) were plated onto LB plates. The as-prepared paper disks were placed at the center of each plate. After 12 h incubation at 37 °C, the zones of bacterial inhibition were measured by a millimeter scale (n = 3).

### 2.6. Cell culture

Human umbilical vein endothelial cells (HUVEC) and human skin fibroblasts (HSFs) were obtained from Hospital of Stomatology, Wuhan University, Human immortalized keratinocytes (HaCaT) (GDC0106) and L929 cells (ATCC CRL-6364) were obtained from China Center for Type Culture Collection (CCTCC). HUVECs and HSFs were cultured in the DMEM medium containing 10% FBS and 1% penicillin–streptomycin. HaCaTs and L929 cells were incubated in the MEM medium containing 10% FBS in the incubator with 5% $CO_2$ at 37 °C.

#### 2.6.1. Cytotoxicity assay

The in vitro cytotoxicity assay was carried out by the MTT assay. L929 cells were seeded under the lower chamber of 24-well transwell (pore size = 0.45 μm, $5 \times 10^4$ cells per well) and cultured in the relevant medium (0.5 mL per well) containing 10% FBS for 24 h. Various CFU (0, $10^7$, $5 \times 10^7$ $10^8$, $5 \times 10^8$, $10^9$) of *R. mucosa* were placed in the upper chamber, respectively. The medium in the upper chamber was removed and replaced with the fresh medium without antibiotics for further 48 h. 50 μL of MTT (5 mg/mL) solution was added into each well and co-incubated for 4 h. Then 750 μL of DMSO was added into each well to dissolve formazan. The absorbance intensity (OD) at 570 nm was measured by microplate reader. Relative cell viability was calculated according to the following formula:

$$\text{Cell viability } (\%) = (OD_{570\ \text{sample}} - OD_{570\ \text{blank}}) / (OD_{570\ \text{control}} - OD_{570\ \text{blank}}) \times 100\% \quad (1)$$

The cytotoxicity test of hydrogel and Hy@Rm was measured using the similar method. Briefly, HaCaTs or L929 cells were seeded in the lower chamber of 24-well transwell (pore size = 0.45 μm, $5 \times 10^4$ cells per well) and cultured in the relevant medium (0.5 mL per well) containing 10% FBS for 24 h at 37 °C. The hydrogel (200 μL per well) or Hy@Rm ($5 \times 10^8$ CFU of *R. mucosa*, 200 μL hydrogel per well) were put into the upper chamber. Meanwhile, the culture media in the lower chamber were removed and replaced with 0.5 mL of the fresh medium without antibiotics and further co-incubated for 24 h at 37 °C before MTT assay.

#### 2.6.2. Optimization of hydrogel composition

For cell migration assay, HaCaTs were seeded into the 24-well transwell at a density of $5 \times 10^4$ cells per well. After 24 h, the lower chambers were scratched by a sterile p200 pipette tip and washed with PBS to remove the unattached cells. The concentration of PVP, PVA and SA solutions (w/v) was fixed at 10%, 10%, and 2%, respectively, Then, 200 μL hydrogels with various compositions (PVP: PVA: SA = 5/5/5, 5/5/4, 5/5/3, 5/5/2, 5/5/1, v/v/v) were placed into the upper transwell (pore size = 8 μm). HaCaTs were photographed by inverted microscope at 0, 24, and 48 h. When the volume ratio of PVP: PVA: SA (v/v/v) was 5:5:3, the migration of HaCaTs was maximal. So, the optimal weight ratio of PVP/PVA/SA was determined as (10% × 5): (10% × 5): (2% × 3) = 25/25/3.

#### 2.6.3. In vitro migration assay

HaCaTs were seeded in 24 well plates at a density of $5 \times 10^4$ cells per well into the lower chamber and cultured for 24 h. Subsequently, the plates were scratched by a sterile p200 pipette tip and washed with sterile PBS to remove unattached cells. Then, the adherent cells were co-incubated with 200 μL of the hydrogel, 200 μL of Hy@Rm ($5 \times 10^8$ CFU of *R. mucosa*), 200 μL of *R. mucosa* ($5 \times 10^8$ CFU) per well into the upper chamber. HaCaTs were photographed by inverted microscope at 0, 24, and 48 h after the scratching treatment. The migration rate was determined by calculating the ratio of the closed area to the initial wound.

#### 2.6.4. Study of pro-proliferating effect on cells

The in vitro cell proliferation assay was performed by the MTT assay. HSFs were seeded into the lower chamber of 24-well transwell with 0.45 μm pore-size filters at a density of $5 \times 10^4$ cells per well with the serum-free medium. The hydrogel (200 μL), *R. mucosa* ($5 \times 10^8$ CFU), and Hy@Rm dressing (200 μL, $5 \times 10^8$ CFU of *R. mucosa*) were placed into the upper chamber and co-incubated with HSF cells for 24 h at 37 °C, respectively. 50 μL of MTT (5 μg/mL) solution was added into each cell well and co-incubated for another 4 h, then 750 μL of DMSO was added into each well to dissolve formazan. Absorbance at 570 nm was measured by microplate reader for cell viability assay.

#### 2.6.5. Tube formation assay

Tube formation assay was conducted according to the reported method [32]. Briefly, 250 μL of the thawed Materigel solution (the mixing ratio of Matrigel relative to the culture medium was 1:2) was added into lower chamber of a pre-cooled 24-well transwell and then incubated for 60 min at 37 °C. Subsequently, HUVECs were seeded into the Materigel-containing lower chamber at a density of $5 \times 10^4$ cells per well and co-incubated with the hydrogel (200 μL), *R. mucosa* ($5 \times 10^8$ CFU), and Hy@Rm dressing (200 μL hydrogel, $5 \times 10^8$ CFU *R. mucosa*) in the upper chamber for 6 h at 37 °C. To evaluate the tube formation, HUVECs were stained with Calcein-AM for the visual observation by the fluorescence inverted microscope and quantified by imageJ software.

### 2.7. Hy@Rm dressing distribution and degradation in vivo

#### 2.7.1. Preparation of Cy7-SA

SA was chemically linked with Cy7-$NH_2$ (Mw = 807.07) under the assistance of EDC and NHS. 2.45 mg ($3.03 \times 10^{-3}$ mmol) of Cy7-$NH_2$ dispersed in 1 mL of DI water was poured into 6 mL of 2% SA solution. Then 234 mg ($1.55 \times 10^{-3}$ mmol) of EDC and 223 mg ($1.55 \times 10^{-3}$ mmol) of NHS dissolved into 1 mL of DI water was added into the above SA solution. The reaction system continued to stir for 24 h and then poured into a large amount of ethyl alcohol to isolate Cy7-SA, which was further purified by repeated washing with ethyl alcohol and drying in vacuum. The procedure was free from light.The prepared SA-Cy7 was suspended in 6 mL of DI water ready for use.

#### 2.7.2. Preparation of Cy5-R. mucosa

50 μL of Cy5-NHS (1 mg/mL) was placed into 1 mL of PBS solution containing $5 \times 10^9$ CFU of *R. mucosa* and the mixture was shaken for 2 h. Then the *R. mucosa* was washed by fresh PBS thrice to obtain Cy5 labeled *R. mucosa* (Cy5-*R. mucosa*).

#### 2.7.3. Preparation of fluorescently labeled Hy@Rm dressing

Cy5-*R. mucosa* were suspended in 1 mL of ice-cold calcium phosphate solution (pH = 4.8) containing 12.5 mM of $CaCl_2$. After vortexing for 5 min, the mixture was added into the solutions of PVP/PVA/Cy7-SA (volume ration at 5/5/3) and further shaken for 10 min to obtain the fluorescently labeled Hy@Rm dressing.

#### 2.7.4. IVIS imaging

Cy5-*R. mucosa* ($5 \times 10^8$ CFU), and the fluorescently labeled Hy@Rm dressing (200 μL of hydrogel, $5 \times 10^8$ CFU of *R. mucosa*) were smeared on the dorsal skins of AD mice. After treatments, the mice were anesthetized and imaged using IVIS imaging system (Cy5, Ex: 646 nm, Ex: 664 nm; Cy7, Ex: 750 nm, Ex: 790 nm) at different time points.

### 2.8. Study of skin diffusion and penetration of Hy@Ru dressing

SA was linked with FITC-PEG-$NH_2$ (Mw = 3400) under the assistance of EDC and NHS to obtain SA-FITC according to the similar route of Cy7-SA preparation as stated above. SA-FITC was dissolved in DI water ready for use. Also, the preparation of PVP/PVA/SA/$Ca^{2+}$-FITC hydrogel was similar to that of PVP/PVA/SA/$Ca^{2+}$ hydrogel. Dorsal skin tissues of mice were used for penetration study. A PVP/PVA/SA/$Ca^{2+}$-FITC hydrogel containing Cy5-*R. mucosa* was smeared on dorsal skin tissues. After 12 h, skin tissues were collected and fixed with 4% paraformaldehyde for slice analysis.

### 2.9. Establishment of DNCB-induced AD mice model and in vivo therapy evaluations

Female Balb/c mice (6–8 weeks old) were obtained from the Animal Biosafety Level III Lab, Wuhan University. All of the animal experiments were conducted under protocols approved by the Institutional Animal Care and Use Committee (IACUC) of the Animal Experiment Center of Wuhan University (Wuhan, China). The mice were subjected to hair removal before AD model induction. AD mice were induced by topical administration with 1% DNCB in 200 μL of acetone/olive oil mixture (v/v, 2:1) per mouse on the dorsal skin thrice (every two days) at the first week. Then, 200 μL of 0.5% DNCB were applied twice each week for 6 weeks. Mice were randomly divided into 5 groups (n = 5): normal group (normal mice without any treatments), untreated group (AD mice without any treatment), Hy group (AD mice treated with the hydrogel), Rm group (AD mice treated with *R. mucosa*) and Hy@Rm group (AD mice treated with Hy@Rm dressing).

Specifically, hydrogel (200 μL per mice), *R. mucosa* ($5 \times 10^8$ CFU per mice), and Hy@Rm dressing (200 μL hydrogel, $5 \times 10^8$ CFU of *R. mucosa* per mice) were applied on dorsal skin of AD mice thrice a week for 6 weeks. During treatments, the body weight was recorded once a week. Moreover, the dermatitis score was evaluated as the sum of scores according to the classification [33]: 0 (no symptoms), 1 (mild), 2 (moderate) and 3 (severe), following five signs and symptoms: (1) erythema/hemorrhage, (2) scarring/dryness, (3) edema, (4) excoriation/erosion, and (5) lichenification. TEWL, skin hydration, and skin elasticity were assessed on day 0, 7, 14, 21, 28, 35, and 42 before each administration of DNCB. Scratching behavior of each group was recorded in an hour by video. Before the observation over scratching behavior, AD mice were individually isolated for 30 min. After 6 weeks, mice were euthanatized to collect skin tissues, spleen, and blood. Dorsal skin tissues were collected and fixed with 4% paraformaldehyde for 48 h. Then the tissues were stained with hematoxylin and eosin (H&E), tobuidine blue (TB), and masson stain for slice analysis, and the blood was measured by ELISA and blood biochemistry and blood routine analysis.

### 2.10. Colonization assay in vivo

Mice were sacrificed after 6-week treatments and the dorsal skin tissues were harvested. The skin tissues were weighed and cut up. Then, the skin tissues were grinded up, resuspended in PBS to dilute to different concentrations. 100 μL of the diluted solution was plated evenly on R2A plates (containing 300 μg/mL vancomycin and 5 μg/mL amphotericin B) and Chromogenic *Staph aureus* Agar plates, respectively. After incubation for 48 h, the number of bacterial colonies were calculated by the plate-count method.

## 3. Results and discussion

### 3.1. Preparation and characterization of Hy@Rm dressing

Patients with AD is rather deficient in Gram-negative microbiota on the diseased skins compared with healthy population [34]. Normal skins are colonized by more gram-negative bugs that play protective roles by producing necessary peptides or lipids [35]. *R. mucosa*, one of the most common species from healthy skin, is able to inhibit *S. aureus* growth, but their efficacy of in vivo AD treatments suffers from the competitive suppression by *S. aureus* that predominantly colonize AD sites [14]. The major aim of this study is to solve this significant challenge.

We isolated *R. mucosa* from the healthy volunteers and cultured it under the optimized conditions [36]. The *R. mucosa* strain was verified by morphological observation (Fig. S1) and strain identification via polymerase chain reaction (PCR) sequence analysis (Tables S1–S2). The construction of Hy@Rm dressing relied on the calcium ions mediated electrostatic crosslinking among *R. mucosa*, PVP, PVA and SA. PVP and PVA have been widely used as restorative materials because they offer a physiologically benign environment for cell proliferation and migration [37–40]. In addition, PVA is up to date the only one among vinyl polymers suited as a carbon and energy source for bacteria [41–43]. SA has been intensively utilized for medical applications such as wound dressings, scaffolds, and surgical impression materials [44,45]. To integrate the three polymers with *R. mucosa* into a dressing agent, PVP, PVA and SA were first fused together by the freezing-thawing cycle method to obtain PVP/PVP/SA matrix. Because the wound healing depends largely on the migration and growth of keratinocytes [46], a series of PVP/PVA/SA hydrogels were prepared at various feeding ratios for the optimization according to the migration of human immortalized keratinocytes cell (HaCaT) (Figs. S2a–S2b). Based on the result, the optimal weight ratio of PVP/PVA/SA was determined as 25:25:3.

Next, calcium ions were anchored onto the negatively charged surface of *R. mucosa* as the cross-linking sites to permit the stable embedding of *R. mucosa* into PVP/PVP/SA matrix to give Hy@Rm dressing [47,48]. For comparison, the bacteria-free hydrogel (Hy) of PVP/PVP/SA/$Ca^{2+}$ was prepared in the similar way. Observation by scanning electron microscopy (SEM) verified that the polymers were inter-entangled into a network while *R. mucosa* bacteria were evenly embedded in the Hy@Rm dressing (Fig. 1a). The rheological properties of Hy were investigated in the presence/absence of *R. mucosa* (Fig. 1b). Introduction of *R. mucosa* into Hy@Rm led to a significant increase of the damping factors (Tanδ) [49]. These results indicated that *R. mucosa* was successfully fused together with the hydrogel matrix.

High biosafety is the prerequisite for the practical application of therapeutics in vivo. 3-(4,5-dimethylthiazol-2-yl)-2,5-diphenyltetrazolium bromide (MTT) assay was conducted to evaluate the biocompatibility of Hy@Rm dressing in cellular levels. *R. mucosa* showed high bio-security toward L929 cells after 48 h co-incubation (Fig. S2c). The proliferation of L929 cells was not affected and even boosted in the presence of *R. mucosa* because *R. mucosa* is a kind of commensal skin bacteria. As shown in Fig. 1c and Fig. 1d, cellular co-

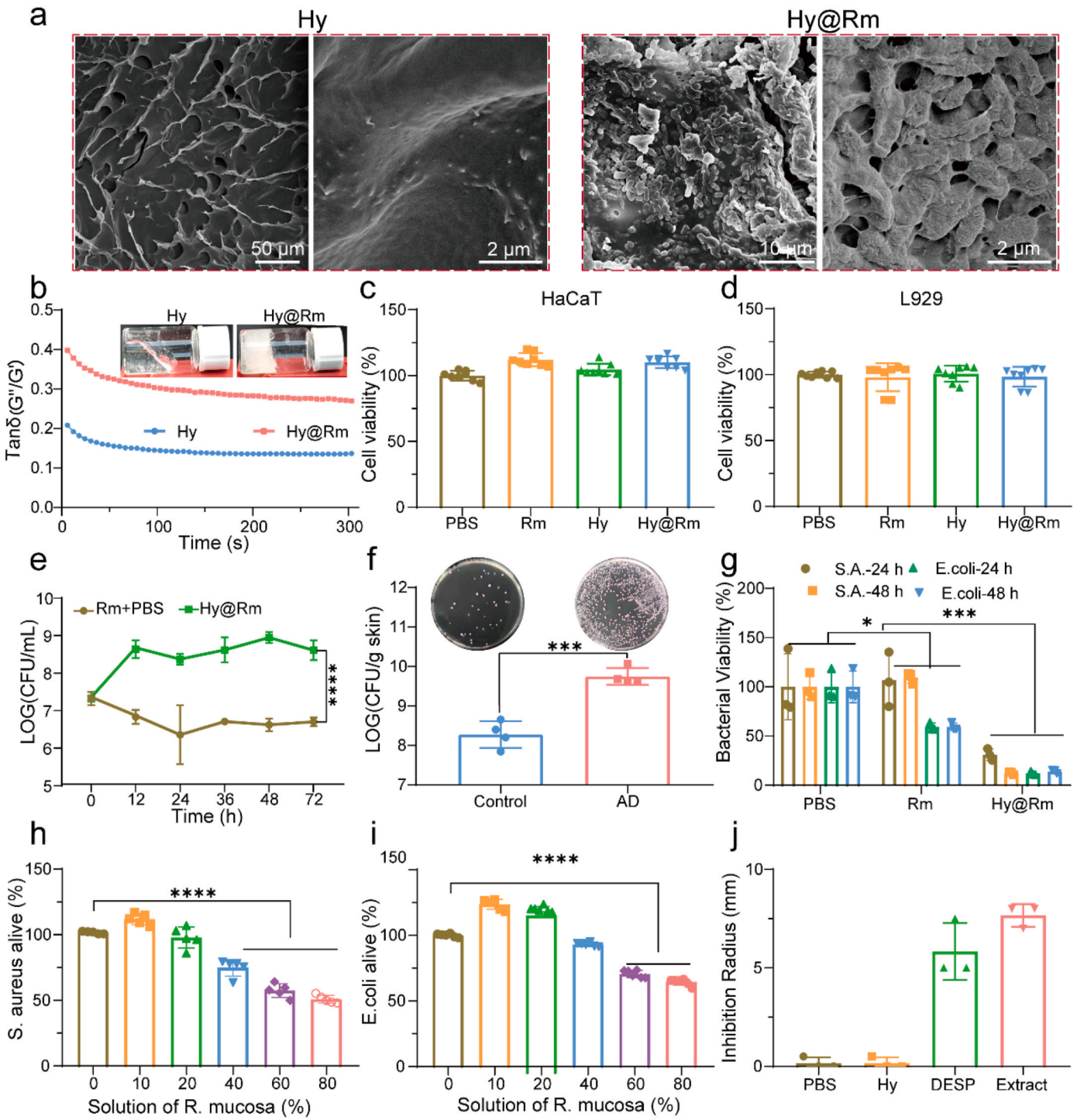


**Fig. 1.** Characterization of Hy@Rm dressing. a) SEM image of the Hy and Hy@Rm. b) Photographs and viscoelasticity of Hy@Rm dressing (G′, G″, and Tan δ means storage modulus, loss modulus, and damping factor respectively, Tan δ = G''/G′). c) Cell viability of HaCaT and (d) L929 cells co-incubated with Hy@Rm dressing for 24 h. e) *R. mucosa* viability in Hy@Rm dressing in comparison with that of bare *R. mucosa* in PBS at 37 °C. f) Images and quantification of *S. aureus* in healthy and AD mice (n = 4). Bacterial colonies of *S. aureus* appear in pink or purple color. g) Bacterial viability of *E. coli* and *S. aureus* in bacterial antagonism experiment (n = 3). h) and i) Antibacterial activity of the culture medium of *R. mucosa* with different concentrations. j) Antimicrobial activity of the *R. mucosa* extract (8 mg/ml), the hydrogel and sphingolipid DESP (0.17 mg/mL) against *S. aureus* (n = 3). Significance between every two groups in Fig. (1e) was calculated using unpaired two-way ANOVA and in Fig. (1f) by students unpaired *t*-test, and in Fig. (1g-i) *via* one-way ANOVA with Tukey post-hoc analysis, respectively. Data were shown as mean values ± standard deviation (SD). (*p < 0.05, **p < 0.01, ***p < 0.001, and ****p < 0.0001.

incubation with Hy and Hy@Rm exerted nearly no influences on the survival of both HaCaT and L929 cells.

### 3.2. Antimicrobial capability of Hy@Rm dressing in vitro

Hy@Rm was arranged to function as not only culture harbors but also as polymeric nutrients to support the growth of the embedded *R. mucosa* in the harsh microenvironment of AD sites. The bacterial

viability in phosphate buffer solution (PBS) was examined by the plate-count method. The CFU apparently dropped over time in the group of bare *R. mucosa* (Fig. 1e). In contract, the *R. mucosa* in Hy@Rm dressing gradually proliferated and the CFU values were even two magnitudes higher than that of bare *R. mucosa*, suggesting the positive contribution of polymeric matrix, such as the nutrients supply for bacterial survival. In addition, the viability of *R. mucosa* in Hy@Rm was significantly improved compared with free *R. mucosa* at clinically relevant temperatures (RT, 4 °C, −20 °C) (Fig. S3a). To probe the underlying mechanism, we explored the influence of each component in Hy@Rm dressing on bacterial growth. As shown in Fig. S3b, all the three polymers (PVP, PVA and SA) could more or less boost bacterial proliferation. It has been documented that *S. aureus* tends to predominately colonize AD lesions in the microbial community, which has strong association with AD progression. Compared with healthy mice, AD mice models actually presented a considerable elevation of *S. aureus* units (Fig. 1f). We compared the bacterial antagonism of Hy@Rm dressing and bare *R. mucosa* against pathogenic bacteria. A dose of $10^7$ CFU of *S. aureus* or *E. coli* was put into the fresh medium. Hy@Rm dressing and bare *R. mucosa* were then added with the same dosage of *R. mucosa*, respectively. The result manifested that both of Hy@Rm dressing and bare *R. mucosa* could inhibit the proliferation of *E. coli*, but the former displayed much stronger activity (Fig. 1g). It is noted that bare *R. mucosa* affected insignificantly the proliferation of *S. aureus* in contrast to the evident inhibition effect as detected for Hy@Rm. Apparently, *R. mucosa* alone was difficult to compete with *S. aureus,* but its dressing form of Hy@Rm could largely boost its competition capability in the presence of *S. aureus.* The result agreed well with the clinically poor outcome of *R. mucosa* in treating AD disease, and it also adumbrated the feasibility of Hy@Rm to overcome the biological barrier for the microbiome-based AD biotherapy caused by the indigenous pathogens.

We speculated that the inhibited proliferation of pathogenic *S. aureus* may have association with the substances secreted by the coexisting *R. mucosa* in addition to the competition among different bacterial sources. Hence, after *R. mucosa* was cultured for 48 h, the culture medium was isolated and diluted with different amounts of fresh medium for the following culture of *S. aureus* and *E. coli*. The *R. mucosa*-free fresh medium was used as the negative control. The results verified our speculation, showing that the antibacterial activity against *S. aureus* and *E. coli* was enhanced as increasing the proportion of the *R. mucosa* culture medium in the diluents (Fig. 1h and Fig. 1i). Apparently, *R. mucosa* could secrete certain substances to inhibit the proliferation of *S. aureus*, though this effect may be largely compromised when the two bacteria were co-cultured due to the antagonism between bacteria from different sources. Studies have reported that *R. mucosa* could produce sphingolipids metabolites such as sphingomyelins, ceramides, phospholipids, and arachidonic acid, which are known as natural antimicrobial agents [50,51]. Liquid chromatography coupled with tandem mass spectrometry (LC-MS/MS) was performed to analyze the extract obtained from 50 mL of the *R. mucosa* containing medium ($5 \times 10^8$ CFU/mL) after 48 h culture (Fig. S4, and Fig. S5). The presence of sphingolipid compounds was confirmed by the emergence of $[M+H]^+$ signals of fragment ions at *m/z* 288 (Compound 1), 538 (Compound 2), 380 (Compound 3), and 703 (Compound 4), which belonged to four main sphingolipids as reported [31,52]. When compound 3 of D-erythro-spingosine-1-phospate (DESP) was taken as the reference compound, its content in the extract was quantified at a very high level up to 6.5 μg/mL by LC-MS/MS (Table S3). In addition, the bacterial disk diffusion test was conducted to compare the antibacterial potency between pure DESP and the DESP-containing extract at the same DESP dosage. The obtained data partly reflected that the DESP in the extract played a major role in the antibacterial activity and there might exist other antibacterial substances in the extract (Fig. 1j). Anyway, these results clearly manifested that *R. mucosa* could continuously secrete antibacterial metabolites to inhibit *S. aureus* proliferation, provided that *R. mucosa* could prevent themselves from the elimination by *S. aureus*. At this point, if Hy@Rm dressing offers a benign condition to support the survival of *R. mucosa* in the AD-localized skins, it would enable better efficacy of *R. mucosa*-based microbe therapy toward AD disease.

### 3.3. *In vitro evaluation of Hy@Rm dressing over epithelial regeneration and wound healing*

Since AD disease is accompanied by chronic, inflamed skin lesions and tissue injury, it is preferable that AD therapy could simultaneously benefit epithelial regeneration and wound healing. Hence, we investigated the pro-regenerative and wound-healing capabilities of Hy@Rm dressing under the condition simulating the in vivo environment. Studies have documented that wound healing involves a variety of cellular actions mainly including keratinocyte migration, fibroblast proliferation, and endothelial cell differentiation [53,54]. The corresponding influences of Hy@Rm over human immortalized keratinocytes (HaCaTs), human skin fibroblasts (HSFs) and human umbilical vein endothelial cells (HUVECs) were thus studied (Fig. 2a). The migration of epidermal keratinocytes is critical for epithelial regeneration during wound healing process. The in vitro scratch-wound assay is a typical method to assess their migratory capacity [53]. Compared with the blank control, bare *R. mucosa* mildly facilitated HaCaT migration while such an effect was represented more profoundly in groups of Hy@Rm and Hy (Fig. 2b). The cell amount per migration trace and the migration area were measured to provide quantitative data about HaCaT migration. As shown in Fig. 2c and Fig. S6, significant differences were observed in cell migration between groups of Hy@Rm and bare *R. mucosa.* Using HSF as the model cell, we demonstrated the significantly boosted fibroblast proliferation in Hy@Rm group compared with *R. mucosa* group (Fig. 2d). Endothelial cells play important roles in vascularization during wound healing process [55]. Matrigel tube formation assay was performed to in vitro assess the vessel-forming capability. As shown in Fig. 2e–f, Hy@Rm gave the best outcome in terms of the length and branches of tubes developed by the treated HUVEC, and Hy also displayed positive contribution to angiogenesis. Collectively, these in vitro results adumbrated that our bacteria-involved dressing design would largely benefit epithelial regeneration and wound healing.

### 3.4. *decomposition and penetration of Hy@Rm dressing on skins*

Next, the decomposition and skin penetration of Hy@Rm dressing were investigated in vivo in view of their important roles in colonization of *R. mucosa* on skins. For living imaging, *R. mucosa* was labeled by Cy5 and polymeric matrix was labeled by Cy7, respectively. Hy@Rm and bare *R. mucosa* were deposited on mouse dorsal skin. As shown in Fig. 3a and Fig. S7, the intensity of Cy5 fluorescence representing *R. mucosa* in the group of bare *R. mucosa* gradually dropped and became very weak at 48 h. In Hy@Rm group, Cy5 intensity was always much higher than that of bare *R. mucosa* and still remained at a high level at 48 h. Meanwhile, the intensity of hydrogel-Cy7 fluorescence also had a considerable decline at 48 h after the treatment with Hy@Rm dressing, suggesting the hydrogel decomposition of Hy@Rm dressing on skins. To visualize the tissue penetration, Hy in Hy@Rm dressing was labeled with FITC, and the embedded *R. mucosa* was labeled with Cy5 for ex vivo CLSM observation, which showed that Hy@Rm penetrated through stratum corneum into epidermis region (Fig. 3b). Given that *S. aureus* infection is always restricted to the upper layer of epidermis, the epidermis accumulation of Hy@Rm matched well the character of *S. aureus* infection. Fluorescence In Situ Hybridization (FISH) technique was employed to stain *R. mucosa* strain in skin tissue for CLSM observation after Hy@Rm dressing was deposited on mice skin for 12 h. As shown in Fig. 3c, Hy@Rm tightly adhered onto skin surface with strong fluorescence detected in skin tissue in contrast to the faint fluorescence in the group of bare *R. mucosa*. All these results indicated that Hy@Rm enabled the embedded *R. mucosa* to colonize skin epidermis more readily.

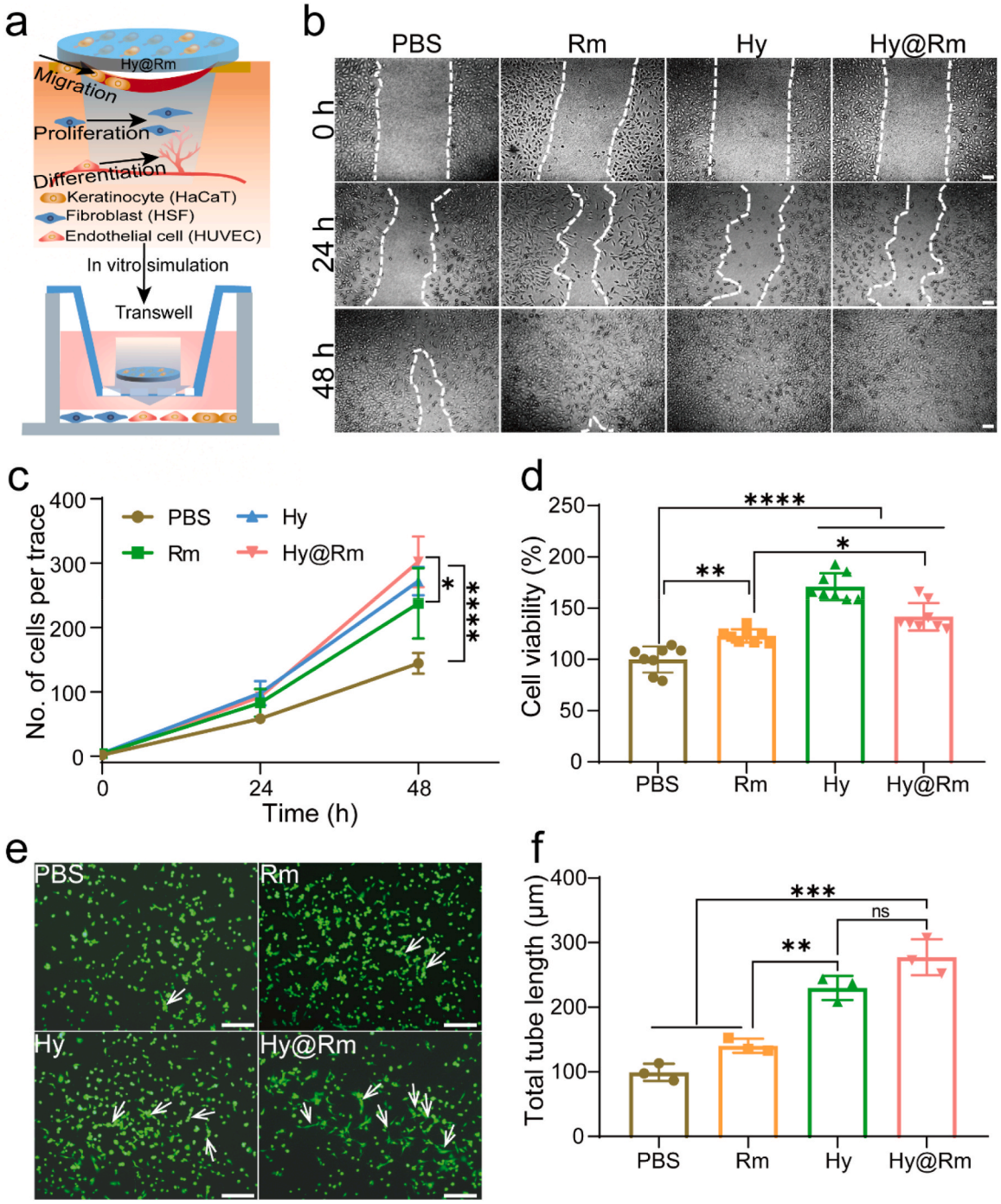


**Fig. 2.** In vitro wound-healing capability of Hy@Rm dressing. a) Illustration of the wound-healing process and experimental design of skin cells treated with Hy@Rm. b) Representative images and c) quantification of HaCaTs in migration experiment (n = 5), Scale bar: 100 μm. d) Quantification of HSF co-incubated with Hy@Rm for 48 h (n = 8). e) Representation images and f) quantification of HUVECs' tube formation for 6 h (n = 3). The tube formation was indicated by white arrows. Scale bar: 200 μm. Significance between every two groups in was calculated using two-way ANOVA in Fig. (2c) and one-way ANOVA with Tukey post-hoc analysis in Fig. (2d, 2f), respectively. Data were presented as mean values ± SD. Images were merged or quantified using Image J software.

### 3.5. Antimicrobial capability of Hy@Rm dressing in vivo

We have demonstrated that Hy@Rm dressing could prolong the retention of the embedded *R. mucosa* on mice skins in vivo and help it combat *S. aureus* in vitro. Theoretically, these benefits would favor the colonization of *R. mucosa* on AD sites, which is challenged by the indigenous pathogenic *S. aureus*. To verify this expectation, we monitored the variation of *R. mucosa* amount over time after the transplant of bare *R. mucosa* and Hy@Rm onto the AD-localized mice skins. *R. mucosa* were collected by swabs from the skins for the plate counting using the gradient dilution method. The amount of *R. mucosa* on skin rapidly dropped with time in the group of bare *R. mucosa*. In comparison, this decreasing trend was dramatically retarded in Hy@Rm group (Fig. 3d–e and Fig. S8). Correspondingly, there appeared a considerable reduction of *S. aureus* on skin of AD mice in Hy@Rm group, indicating the substantial suppression of *S. aureus*. However, such an effect was minimal in groups of bare *R. mucosa* and empty Hy (Fig. 3f and Fig. S9), which agreed well with the in vitro results. Apparently, the artificially

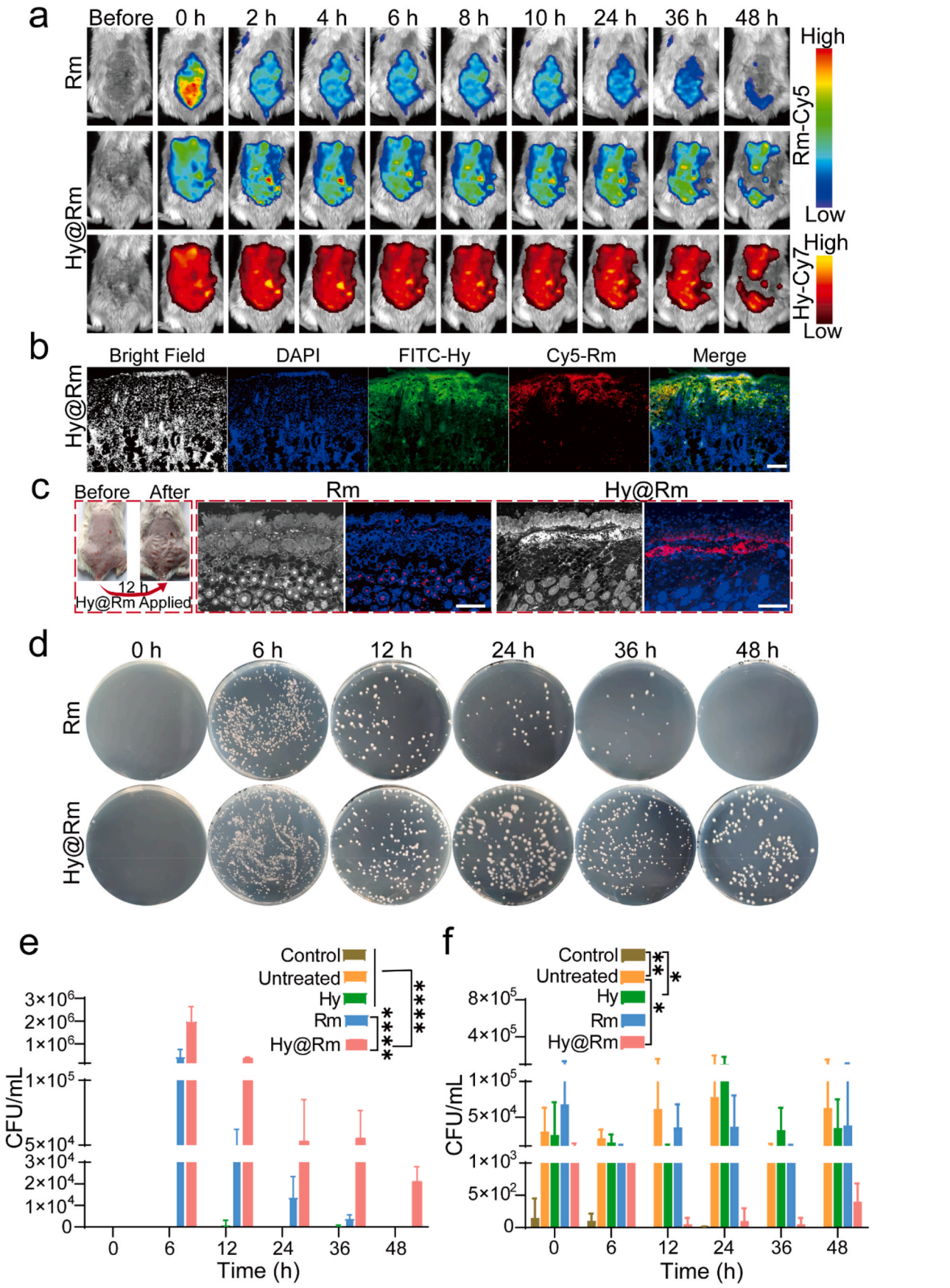


*(caption on next page)*

**Fig. 3.** Decomposition, distribution and antimicrobial abilities of Hy@Rm dressing. a) Decomposition of Hy@Rm dressing on the surfcace of mice skin at different time points. *R. mucosa* was labeled by Cy5, hydrogel was labeled by Cy7. Upper and middle images showed fluorescence intensity of *R. mucosa* in Rm group and Hy@Rm group respectively, and the bottom images displayed the fluorescence intensity of Hy in Hy@Rm group. b) Penetration of Hy@Rm dressing through the stratum corneum at 12 h. The hydrogel was labeled by FITC and *R. mucosa* was labeled by Cy5. The cells were staind by DAPI (Scale bar: 100 μm). c) Left: photograph of Hy@Rm dressing on mose skin at 12 h. Right: Fluorescence In Situ Hybridization in mice skin at 12 h after *R. mucosa* or Hy@Rm dressing were administrated. *R. mucosa* (red) mainly accumulated in the epidermis. The cell was staind blue by DAPI (Scale bar: 100 μm). d) Representative plate coating pictures and e) quantitation of *R. mucosa* taken from mice with AD at different time points (n = 4). f) Quantitation of *S. aureus* by plate dilution method (n = 4). Statistical significance was calculated by two-way ANOVA with Tukey post-hoc analysis in Fig. (3e-f). Data were presented as mean values ± SD.

constructed microenvironment by Hy@Rm dressing, which provided culture harbors and nutrients for *R. mucosa*, is necessarily needed to support the embedded *R. mucosa* to effectively defeat the antagonism of *S. aureus,* thus permitting chances to eliminate *S. aureus.*

### 3.6. In vivo evaluation of AD therapy and wound healing

Considering the relapsing characteristic of AD disease and the self-healing ability of mice, we established the relapsing AD mice model by smearing 2,4-dinitrochlorobenzene (DNCB) on the dorsal skin consecutively for 7 weeks to more accurately assess the therapeutic performance of Hy@Rm dressing in vivo. Hy, bare *R. mucosa*, and Hy@Rm dressing were topically administrated during 6 weeks, respectively (Fig. 4a). As shown in Fig. 4b, DNCB treatment locally induced skin lesions with the typical AD symptoms, including skin dryness, erythema, induration, edema, excoriation, erosion and so on. Empty Hy and Rm (bare *R. mucosa*) showed moderate therapeutic effects, while Hy@Rm alleviated AD symptoms much more effectively. In AD patients, skin barrier destruction is associated with the increase of trans-epidermal water loss (TEWL), and the reduction of skin hydration/elasticity [56]. Regarding these indicators of skin conditions, there appeared an evident improvement of skin status, as evidenced by the remarkably reduced TEWL (Fig. 4c), the increased skin hydration (Fig. 4d), and the enhanced skin elasticity (Fig. 4e) after the treatment with Hy@Rm dressing. By comparison, it is concluded that both bare *R. mucosa* and empty hydrogel exerted favoring effects on skin status. The former was ascribed to the therapeutic effect and the latter was due to its water-preserving ability [57]. Dermatitis score index is the most validated scoring system to reflect AD degrees. After treatments, the dermatitis score values based on erythema/hemorrhages, scarring/-dryness, edema, excoriation/erosion, and lichenification were determined (Table S4) [33]. As expected, the dermatitis score in AD mice was evidently decreased after Hy@Rm treatment at sixth week (Fig. 4f), showing better therapeutic effect than the other groups. During treatments, no significant loss of body weight was detectable for the mice treated by various formulations (Fig. 4g). Pruritus, one of the most significant symptoms of AD, significantly reduce the quality of life [58]. The itching frequency of AD has thus been acknowledged as another important index reflecting the severity of AD disease. Intuitively, the treatment with Hy@Rm could largely alleviated the scratching behavior in AD mice. Hy and Rm also had moderate anti-pruritic effect when compared with the untreated group (Fig. 4h). These results manifested that both Hy and Rm played indispensable roles in the Hy@Rm treatment.

### 3.7. Influences on inflammatory/immune responses caused by Hy@Rm dressing

An imbalance between T-helper cell type 2 (Th2) immune response, which drives allergic responses, and T-helper cell type 1 (Th1) immune response, which is essentially triggered during infections, is evident in AD [59,60]. The immune disorder would considerably affect major organs, particularly the splenomegaly. As shown in Fig. 4i–j, the DNCB-induced mice actually displayed an evident increase in the volume and the weight of spleen organs. Upon the treatment with Hy@Rm, the spleen vol/wt in AD mice were gradually restored to the normal. To deeply understand the protective and pathological immune responses in the untreated and treated AD mice, histological analyses including hematoxylin-eosin (H&E) staining, toluidine blue (TB) staining and masson staining were carried out. As shown in Fig. 5a–c, these analyses manifested the occurrence of notable skin abnormalities in the DNCB-induced AD sites, including epidermal hyperplasia, edema, fibrosis and accumulation of inflammatory cells in the dermis/epidermis region. Among all the tested groups, only Hy@Rm could simultaneously inhibit the AD-caused epidermis thickening, reduce inflammatory cells and normalize collagen in the AD sites (Fig. S10). As demonstrated in vitro, Hy@Rm dressing could facilitate angiogenesis, which was reconfirmed in vivo by the immunohistochemical analysis, showing that Hy@Rm dressing could boost the population of CD31-positive endothelial cells in the skin dermis (Figs. S11a–S11b). Moreover, we explored the immune-related cytokines by enzyme-linked immunosorbent assay (ELISA) and immunohistochemical staining. IgE plays an essential role in allergen-induced inflammatory processes in various atopic diseases such as AD. The expression level of serum IgE thus serves as a critical index of AD. As shown in Fig. 5d, the expression of serum IgE was dramatically down-regulated after Hy@Rm treatment, and moderately reduced by Rm and even empty Hy. Tumor necrosis factor (TNF-α) is an indicator of chronic inflammation. In comparison, only Hy@Rm dressing could down-regulate the expression of TNF-α to a normal level (Fig. 5e). Skin barrier disruption in AD model would induce the immune response of systemic Th2 cells accompanied by the elevated expression of thymic stromal lymphopoietin (TSLP), which was secreted by the keratinocytes of AD patients. AD mice model actually expressed higher TSLP level in serum than normal mice did (Fig. 5f). However, TSLP expression was down-regulated by topical treatment with Hy@Rm dressing. Meanwhile, Hy@Rm dressing was able to effectively inhibit the expression of inflammatory mediators, such as IL-1β, IL-4 and IL-17a, indicating the anti-inflammatory activity. The anti-inflammatory capability of Hy@Rm was also reflected by immunohistochemical staining analysis (Fig. 5g, Figs. S12a–c). All these results verified the strong capability of Hy@Rm dressing in relieving the inflammatory and immune responses implicated in AD diseases, which is favorable for the treatment of AD [61,62]. Overall, our findings in the DNCB-treated mice model suggested that Hy@Rm dressing may be an effective therapeutic agent to make the diverse disorders caused by AD disease to become normalized.

### 3.8. Antibacterial activity of Hy@Rm dressing in vivo

We investigated the competition between *R. mucosa* and *S. aureus* on skin surface of the AD mice model after different treatments. The colonization rate of *R. mucosa* on skins was measured by the serial dilution plating and counting method. The treatment with Hy@Rm dressing apparently boosted the colonization of *R. mucosa* (Fig. 5h). *S. aureus* was quantified using solid positive chromogenic staphylococcus aureus plates via the recognition of pigmented colonies. In consistence with the data about *R. mucosa*, Hy@Rm group had much less *S. aureus* than *R. mucosa* group (Fig. 5i), reconfirming the improvement of microbe-based therapy toward AD disease through our approach.

### 3.9. Biosafety of Hy@Rm dressing

In vivo biosafety of Hy@Rm dressing was assessed since it is a critical requirement for bacteria-involved applications in vivo. As

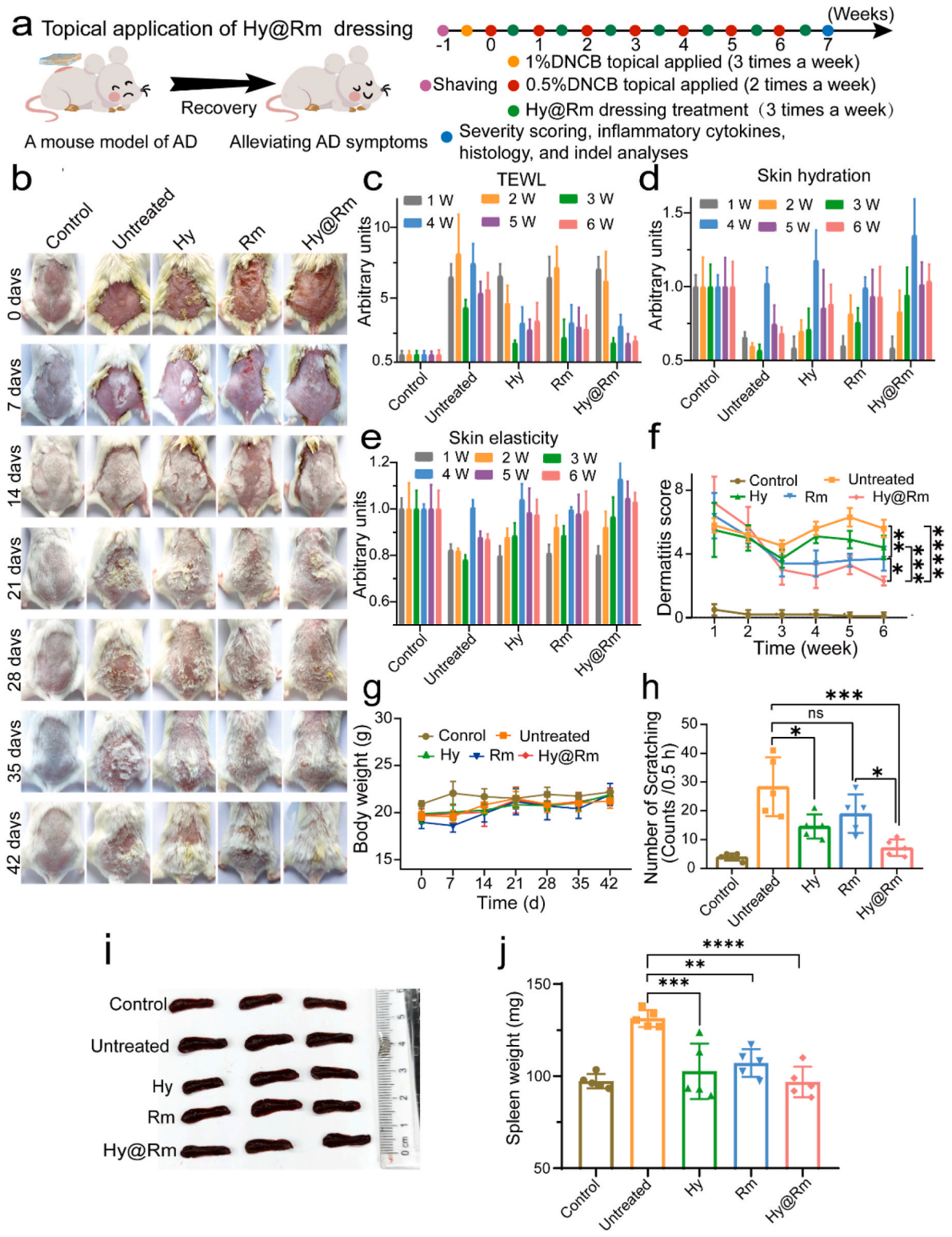


**Fig. 4.** In vivo therapy of DNCB-induced AD by Hy@Rm dressing. a) Schematic illustration of Hy@Rm dressing for treating the DNCB-induced AD mice model. b) Representative photographs of mice with different treatments (n = 5). c) TEWL recorded in various treatments (n = 5). d) Skin hydration and (e) skin elasticity in different groups during the treatments (n = 5). f) Changes in dermatitis score during topical admnistration with various formulations (n = 5). g) Variation of body weight during different treatments. h) Scratching behaviors after different treatments (n = 5). i) Representative photographs of the spleens on day 42 (n = 5). j) Quantitative data of spleen weights on day 42 (n = 5). Statistical significance between every two groups was calculated *via* one-way ANOVA with Tukey post-hoc analysis in Fig. (4h, 4j) and two-way ANOVA with Tukey post-hoc analysis in Fig (4f), respectively. Data were presented as mean values ± SD.

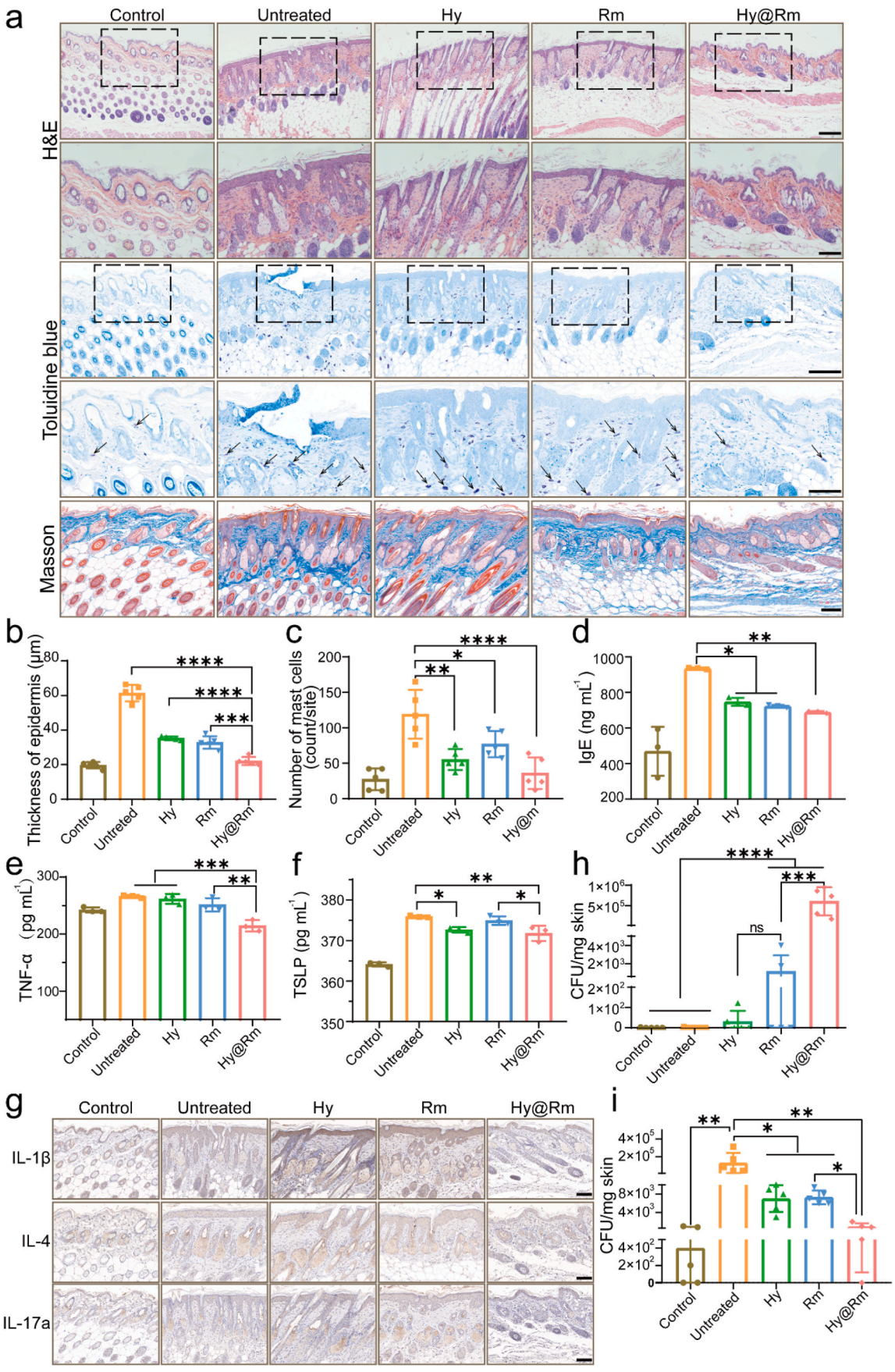


*(caption on next page)*

**Fig. 5.** Histological analyses and colonization outcomes after various treatments. a) Images of tissue slices treated with H&E staining (scale bars: 200 μm and 100 μm), TB staining (scale bars: 200 μm and 100 μm) and masson staining (scale bars: 200 μm). b) Epidermal and dermal thickness measured acccording to H&E-staining images. c) Quantification of mast cells in TB-staining images, mast cell (purple) was indicated by black arrows. d) Serum IgE levels measured by ELISA (n = 3). e) Expression levels of TNF-α determined by ELISA (n = 3). f) Expression levels of TSLP-1 (n = 3). g) Immunohistochemical images of inflammatory factors including IL-1β, IL-4 and IL-17a (scale bars, 100 μm) (n = 3). h) Colonization of *R. mucosa* after various treatments (n = 5). On day 42 skin tissues were taken from euthanatized mice and homogenized and plated by serial dilution. i) Inhibition of *S. aureus* after different treatments (n = 5). Statistical significance in Fig. (5b, 5c, 5d, 5f, 5h, 5i) was calculated via one-way ANOVA with Tukey post-hoc analysis. Data were presented as mean values ± SD.

aforementioned, Hy@Rm treatment didn't cause substantial weight loss during the observation period (Fig. 4g). In addition, Hy@Rm treatment didn't cause abnormal proliferation of *R. mucosa*, and the colony number of *R. mucosa* was decreased over time (Fig. S13). More informations of biosafety were provided from blood biochemistry and blood routine assays (Fig. S14). The result showed that the concentration of white blood cells (WBC), lymphocytes (Lymph), intermediate cells (Mid), granulocyte (Gran), red cells (RBC), and platelets (PLT) exhibited minimal alternations. The enzymes associated with liver function, i.e., alanine transaminase (ALT), aspartate aminotransferase (AST), and gamma-glutamyl transpeptidase (GGT) always kept in a steady levels [25]. Relative to the healthy control, the major kidney function related biomarkers, urea (UREA), glucose (GLU), and creatinine (CRE), showed no significant difference. Furthermore, no noticeable tissue damages were detectable in major organs such as heart, liver, spleen, lung and kidney, as reflected by H&E analysis (Fig. S15). Together with the high cell biocompatibility, all these in vivo results suggested the acceptable biosafety of this bacteria-mediated treatment.

## 4. Conclusion

AD is clinically featured with intense itching, excessive scratching, excoriation, redness, and impaired epidermal barrier function, leading to seriously reduced quality of life. To deal with this troublesome disease, we constructed a living bacterial dressing (Hy@Rm) that delicately integrated the skin symbiotic bacteria of *R. mucosa* into polymeric matrix. Hy@Rm dressing is allowed to not only serve as culture harbors but also nutrients suppliers to support *R. mucosa* survival in the harsh microenvironment of AD sites to combat pathogenic *S. aureus,* which predominantly colonize AD sites. This elaborate design enabled exotic *R. mucosa* to colonize the diseased sites under the strong antagonism of indigenous *S. aureus* and to penetrate in epidermis to inhibit *S. aureus* proliferation mainly by secreting sphingolipids metabolites like a therapeutics bio-factory, whereas *R. mucosa* alone failed when challenged by *S. aureus*. Meanwhile, Hy@Rm dressing could accelerate wound healing, normalize aberrant skin characters, recover skin barrier function, alleviate AD-associated immune responses and inflammations, which behaved like a combinational therapy. This study offers a promising means for the topical bacteria transplant to realize effective microbe therapy toward the skin diseases feature with microbe milieu disorders, including but not limited to AD disease.

## CRediT authorship contribution statement

**Xinhua Liu:** Data curation, Formal analysis, Writing- original draft, Investigation. **Youteng Qin:** Data curation, Methodology, Formal analysis. **Liyun Dong:** and. **Ziyi Han:** Data curation, Formal analysis, Validation. **Tianning Liu:** Data curation. **Ying Tang:** and. **Yun Yu:** and. **Jingjie Ye:** Data curation, Validation. **Juan Tao:** Resources, Methodology. **Xuan Zeng:** Writing – review & editing. **Jun Feng:** Revising, Resource, Writing – review & editing. **Xian-Zheng Zhang:** Supervision, Funding acquisition, Resource, Revising, Writing – review & editing.

## Declaration of competing interest

The authors declare the following financial interests/personal relationships which may be considered as potential competing interests: Jun Feng reports financial support was provided by National Natural Science Foundation of China. Xian-Zheng Zhang reports financial support was provided by National Natural Science Foundation of China. Jun Feng reports financial support was provided by Fundamental Research Funds for the Central Universities.

## Acknowledgement

This work was financially supported by the National Natural Science Foundation of China (52131302, 51973164, 22135005 and 51833007) and the Fundamental Research Funds for the Central Universities (2042021kf0037). All of the animal experiments were conducted under protocols (AUP, WP20210510) approved by the Institutional Animal Care and Use Committee (IACUC) of the Animal Experiment Center of Wuhan University (Wuhan, China).

## Appendix A. Supplementary data

Supplementary data to this article can be found online at https://doi.org/10.1016/j.bioactmat.2022.08.019.

## References

[1] D. Ambrożej, K. Kunkiel, K. Dumycz, W. Feleszko, The use of probiotics and bacteria-derived preparations in topical treatment of atopic dermatitis—a systematic review, J. Allergy Clin. Immunol. Pract. 9 (1) (2021) 570–575, e2.
[2] M.R. Williams, S.K. Costa, L.S. Zaramela, S. Khalil, D.A. Todd, H.L. Winter, J. A. Sanford, A.M. O'Neill, M.C. Liggins, T. Nakatsuji, Quorum sensing between bacterial species on the skin protects against epidermal injury in atopic dermatitis, Sci. Transl. Med. 11 (490) (2019).
[3] S.K. Bantz, Z. Zhu, T. Zheng, The atopic march: progression from atopic dermatitis to allergic rhinitis and asthma, Cell. Immunol. 5 (2) (2014).
[4] I.A. Myles, K.W. Williams, J.D. Reckhow, M.L. Jammeh, N.B. Pincus, I. Sastalla, D. Saleem, K.D. Stone, S.K. Datta, Transplantation of human skin microbiota in models of atopic dermatitis, JCI insight 1 (10) (2016).
[5] J.A. Geoghegan, A.D. Irvine, T.J. Foster, Staphylococcus aureus and atopic dermatitis: a complex and evolving relationship, Trends Microbiol. 26 (6) (2018) 484–497.
[6] A.L. Byrd, C. Deming, S.K. Cassidy, O.J. Harrison, W.-I. Ng, S. Conlan, , N. C. S. Program, Y. Belkaid, J.A. Segre, H.H. Kong, Staphylococcus aureus and Staphylococcus epidermidis strain diversity underlying pediatric atopic dermatitis, Sci. Transl. Med. 9 (397) (2017), eaal4651.
[7] H.H. Kong, J. Oh, C. Deming, S. Conlan, E.A. Grice, M.A. Beatson, E. Nomicos, E. C. Polley, H.D. Komarow, P.R. Murray, Temporal shifts in the skin microbiome associated with disease flares and treatment in children with atopic dermatitis, Genome Res. 22 (5) (2012) 850–859.
[8] J.T. Huang, M. Abrams, B. Tlougan, A. Rademaker, A.S. Paller, Treatment of Staphylococcus aureus colonization in atopic dermatitis decreases disease severity, Pediatrics 123 (5) (2009) e808–e814.
[9] J.E. Greb, A.M. Goldminz, J.T. Elder, M.G. Lebwohl, D.D. Gladman, J.J. Wu, N. N. Mehta, A.Y. Finlay, A.B. Gottlieb, Psoriasis, Nat. Rev. Dis. Prim. 2 (2016), 16082.
[10] S. Weidinger, L.A. Beck, T. Bieber, K. Kabashima, A.D. Irvine, Atopic dermatitis, Nat. Rev. Dis. Prim. 4 (1) (2018) 1.
[11] K. Welsch, J. Holstein, A. Laurence, K. Ghoreschi, Targeting JAK/STAT signalling in inflammatory skin diseases with small molecule inhibitors, Eur. J. Immunol. 47 (7) (2017) 1096–1107.
[12] N. Foolad, A. Armstrong, Prebiotics and probiotics: the prevention and reduction in severity of atopic dermatitis in children, Benef. Microbes 5 (2) (2014) 151–160.
[13] F. Meneghin, V. Fabiano, C. Mameli, G.V. Zuccotti, Probiotics and atopic dermatitis in children, Pharmaceuticals 5 (7) (2012) 727–744.
[14] I.A. Myles, C.R. Castillo, K.D. Barbian, K. Kanakabandi, K. Virtaneva, E. Fitzmeyer, M. Paneru, F. Otaizo-Carrasquero, T.G. Myers, T.E. Markowitz, Therapeutic responses to Roseomonas mucosa in atopic dermatitis may involve lipid-mediated TNF-related epithelial repair, Sci. Transl. Med. 12 (560) (2020) eaaz8631.
[15] I.A. Rather, V.K. Bajpai, S. Kumar, J. Lim, W.K. Paek, Y.-H. Park, Probiotics and atopic dermatitis: an overview, Front. Microbiol. 7 (2016) 507.
[16] T. Nakatsuji, T. Chen, S. Narala, K. Chun, A. Two, T. Yun, F. Shafiq, P. Kotol, A. Bouslimani, A. Melnik, Antimicrobials from human skin commensal bacteria

protect against Staphylococcus aureus and are deficient in atopic dermatitis, Sci. Transl. Med. 9 (2017), eaah4680.
[17] Y. Ito, T. Sasaki, Y. Li, T. Tanoue, Y. Sugiura, A.N. Skelly, W. Suda, Y. Kawashima, N. Okahashi, E. Watanabe, Staphylococcus cohnii is a potentially biotherapeutic skin commensal alleviating skin inflammation, Cell Rep. 35 (4) (2021), 109052.
[18] E.H. Tham, E. Koh, J.E. Common, I.Y. Hwang, Biotherapeutic approaches in atopic dermatitis, Biotechnol. J. 15 (10) (2020), 1900322.
[19] A.J. Hendricks, B.W. Mills, V.Y. Shi, Skin bacterial transplant in atopic dermatitis: knowns, unknowns and emerging trends, J. Dermatol. Sci. 95 (2) (2019) 56–61.
[20] T. Bieber, Atopic dermatitis: an expanding therapeutic pipeline for a complex disease, Nat. Rev. Drug Discov. 21 (1) (2022) 21–40.
[21] Y. Liu, D.Q. Tran, J.M. Rhoads, Probiotics in disease prevention and treatment, J. Clin. Pharmacol. 58 (2018) S164–S179.
[22] E.A. Grice, J.A. Segre, The skin microbiome, Nat. Rev. Microbiol. 9 (4) (2011) 244–253.
[23] M. Rondanelli, M.A. Faliva, S. Perna, A. Giacosa, G. Peroni, A.M. Castellazzi, Using probiotics in clinical practice: where are we now? A review of existing meta-analyses, Gut Microb. 8 (6) (2017) 521–543.
[24] Y. Tang, Q.-X. Huang, D.-W. Zheng, Y. Chen, L. Ma, C. Huang, X.-Z. Zhang, Engineered Bdellovibrio bacteriovorus: a countermeasure for biofilm-induced periodontitis, Mater. Today 53 (2022) 71–83.
[25] Q.W. Chen, X.H. Liu, J.X. Fan, S.Y. Peng, J.W. Wang, X.N. Wang, C. Zhang, C.J. Liu, X.Z. Zhang, Self-mineralized photothermal bacteria hybridizing with mitochondria-targeted metal–organic frameworks for augmenting photothermal tumor therapy, Adv. Funct. Mater. 30 (14) (2020), 1909806.
[26] D.-W. Zheng, P. Pan, K.-W. Chen, J.-X. Fan, C.-X. Li, H. Cheng, X.-Z. Zhang, An orally delivered microbial cocktail for the removal of nitrogenous metabolic waste in animal models of kidney failure, Nat. Biomed. Eng. 4 (9) (2020) 853–862.
[27] Z.-y. Han, X.-f. Bai, Y.-z. Wang, Q.-w. Chen, X.-z. Zhang, Gut microbial glucuronidase-responsive glycyrrhizin micelles for enhanced colon cancer chemotherapy, Acta Polym. Sin. 53 (6) (2022) 626–635.
[28] A. Rodrigo-Navarro, S. Sankaran, M.J. Dalby, A. del Campo, M. Salmeron-Sanchez, Engineered living biomaterials, Nat. Rev. Mater. 6 (12) (2021) 1175–1190.
[29] J.A. Frank, C.I. Reich, S. Sharma, J.S. Weisbaum, B.A. Wilson, G.J. Olsen, Critical evaluation of two primers commonly used for amplification of bacterial 16S rRNA genes, Appl. Environ. Microbiol. 74 (8) (2008) 2461–2470.
[30] N.A. Peppas, S.R. Stauffer, Reinforced uncrosslinked poly (vinyl alcohol) gels produced by cyclic freezing-thawing processes: a short review, J. Contr. Release 16 (3) (1991) 305–310.
[31] C. Chalfant, M. Del Poeta, Sphingolipids as Signaling and Regulatory Molecules, Springer Science & Business Media, 2011.
[32] H. Chen, Y. Cheng, J. Tian, P. Yang, X. Zhang, Y. Chen, Y. Hu, J. Wu, Dissolved oxygen from microalgae-gel patch promotes chronic wound healing in diabetes, Sci. Adv. 6 (20) (2020) eaba4311.
[33] H.-Y. Song, W.S. Kim, S. Mushtaq, J.M. Park, S.-H. Choi, J.-W. Cho, S.-T. Lim, E.-B. Byun, A novel chrysin derivative produced by gamma irradiation attenuates 2, 4-dinitrochlorobenzene-induced atopic dermatitis-like skin lesions in Balb/c mice, Food Chem. Toxicol. 128 (2019) 223–232.
[34] Y. Yamazaki, Y. Nakamura, G. Núñez, Role of the microbiota in skin immunity and atopic dermatitis, Allergol. Int. 66 (4) (2017) 539–544.
[35] J. Abbasi, Are bacteria transplants the future of eczema therapy? JAMA 320 (11) (2018) 1094–1095.
[36] I.A. Myles, J.D. Reckhow, K.W. Williams, I. Sastalla, K.M. Frank, S.K. Datta, A method for culturing Gram-negative skin microbiota, BMC Microbiol. 16 (1) (2016) 1–6.
[37] M.T. Razzak, D. Darwis, Irradiation of polyvinyl alcohol and polyvinyl pyrrolidone blended hydrogel for wound dressing, Radiat. Phys. Chem. 62 (1) (2001) 107–113.
[38] N. Shankhwar, M. Kumar, B.B. Mandal, P. Robi, A. Srinivasan, Electrospun polyvinyl alcohol-polyvinyl pyrrolidone nanofibrous membranes for interactive wound dressing application, J. Biomater. Sci. Polym. Ed. 27 (3) (2016) 247–262.
[39] W. Hu, Y.-W. Su, Y.-K. Jiang, W.-D. Fan, S.-Y. Cheng, Z.-Z. Tong, C. Cen, G.-H. Jiang, Polymer vesicles with upper critical solution temperature for near-infrared light-triggered transdermal delivery of metformin in diabetic rats, Chin. J. Polym. Sci. (2021) 1–9.
[40] Y. Sun, J. Liu, H. Wang, S. Li, X. Pan, B. Xu, H. Yang, Q. Wu, W. Li, X. Su, NIR laser-triggered microneedle-based liquid band-aid for wound Care, Adv. Funct. Mater. (2021), 2100218.
[41] Y. Tokiwa, G. Kawabata, A. Jarerat, A modified method for isolating poly (vinyl alcohol)-degrading bacteria and study of their degradation patterns, Biotechnol. Lett. 23 (23) (2001) 1937–1941.
[42] F. Kawai, X. Hu, Biochemistry of microbial polyvinyl alcohol degradation, Appl. Microbiol. Biotechnol. 84 (2) (2009) 227–237.
[43] T. Vaclavkova, J. Ruzicka, M. Julinova, R. Vicha, M. Koutny, Novel aspects of symbiotic (polyvinyl alcohol) biodegradation, Appl. Microbiol. Biotechnol. 76 (4) (2007) 911–917.
[44] R.W.M. Ng, Y.L. Cheng, Calcium alginate dressing–related hypercalcemia, J. Burn Care Res. 28 (1) (2007) 203–204.
[45] J.O. Kim, J.K. Park, J.H. Kim, S.G. Jin, C.S. Yong, D.X. Li, J.Y. Choi, J.S. Woo, B. K. Yoo, W.S. Lyoo, Development of polyvinyl alcohol–sodium alginate gel-matrix-based wound dressing system containing nitrofurazone, Int. J. Pharm. 359 (1–2) (2008) 79–86.
[46] A.-R.C. Lee, H. Leem, J. Lee, K.C. Park, Reversal of silver sulfadiazine-impaired wound healing by epidermal growth factor, Biomaterials 26 (22) (2005) 4670–4676.
[47] F. Seidi, W.-F. Zhao, H.-N. Xiao, Y.-C. Jin, M.R. Saeb, C.-S. Zhao, Advanced surfaces by anchoring thin hydrogel layers of functional polymers, Chin. J. Polym. Sci. 39 (1) (2021) 14–34.
[48] S.K. Papageorgiou, E.P. Kouvelos, E.P. Favvas, A.A. Sapalidis, G.E. Romanos, F. K. Katsaros, Metal–carboxylate interactions in metal–alginate complexes studied with FTIR spectroscopy, Carbohydr. Res. 345 (4) (2010) 469–473.
[49] S. Fu, A. Thacker, D.M. Sperger, R.L. Boni, I.S. Buckner, S. Velankar, E.J. Munson, L.H. Block, Relevance of rheological properties of sodium alginate in solution to calcium alginate gel properties, AAPS PharmSciTech 12 (2) (2011) 453–460.
[50] J. Arikawa, M. Ishibashi, M. Kawashima, Y. Takagi, Y. Ichikawa, G. Imokawa, Decreased levels of sphingosine, a natural antimicrobial agent, may be associated with vulnerability of the stratum corneum from patients with atopic dermatitis to colonization by Staphylococcus aureus, J. Invest. Dermatol. 119 (2) (2002) 433–439.
[51] N. Bhattacharya, W.J. Sato, A. Kelly, G. Ganguli-Indra, A.K. Indra, Epidermal lipids: key mediators of atopic dermatitis pathogenesis, Trends Mol. Med. 25 (6) (2019) 551–562.
[52] R. t'Kindt, L. Jorge, E. Dumont, P. Couturon, F. David, P. Sandra, K. Sandra, Profiling and characterizing skin ceramides using reversed-phase liquid chromatography–quadrupole time-of-flight mass spectrometry, Anal. Chem. 84 (1) (2012) 403–411.
[53] X. Zheng, S. Narayanan, V.G. Sunkari, S. Eliasson, I.R. Botusan, J. Grünler, A. I. Catrina, F. Radtke, C. Xu, A. Zhao, Triggering of a Dll4–Notch1 loop impairs wound healing in diabetes, Proc. Natl. Acad. Sci. U.S.A. 116 (14) (2019) 6985–6994.
[54] S. Nour, N. Baheiraei, R. Imani, M. Khodaei, A. Alizadeh, N. Rabiee, S.M. Moazzeni, A review of accelerated wound healing approaches: biomaterial-assisted tissue remodeling, J. Mater. Sci. Mater. Med. 30 (10) (2019) 1–15.
[55] C. Liu, X. Cui, T.M. Ackermann, V. Flamini, W. Chen, A.B. Castillo, Osteoblast-derived paracrine factors regulate angiogenesis in response to mechanical stimulation, Integr. Biol. 8 (7) (2016) 785–794.
[56] A. Cristaudo, F. Pigliacelli, F. Sperati, D. Orsini, N. Cameli, A. Morrone, M. Mariano, Instrumental evaluation of skin barrier function and clinical outcomes during dupilumab treatment for atopic dermatitis: an observational study, Skin Res. Technol. 27 (5) (2021) 810–813.
[57] M. Breternitz, D. Kowatzki, M. Langenauer, P. Elsner, J. Fluhr, Placebo-controlled, double-blind, randomized, prospective study of a glycerol-based emollient on eczematous skin in atopic dermatitis: biophysical and clinical evaluation, Skin Pharmacol. Physiol. 21 (1) (2008) 39–45.
[58] M. Fujii, K. Takeuchi, Y. Umehara, M. Takeuchi, T. Nakayama, S. Ohgami, E. Asano, T. Nabe, S. Ohya, Barbiturates enhance itch-associated scratching in atopic dermatitis mice: a possible clue to understanding nocturnal pruritus in atopic dermatitis, Eur. J. Pharmacol. 836 (2018) 57–66.
[59] D. Simon, C. Aeberhard, Y. Erdemoglu, H.U. Simon, Th17 cells and tissue remodeling in atopic and contact dermatitis, Allergy 69 (1) (2014) 125–131.
[60] T. Dainichi, A. Kitoh, A. Otsuka, S. Nakajima, T. Nomura, D.H. Kaplan, K. Kabashima, The epithelial immune microenvironment (EIME) in atopic dermatitis and psoriasis, Nat. Immunol. 19 (12) (2018) 1286–1298.
[61] N. Shershakova, E. Baraboshkina, S. Andreev, D. Purgina, I. Struchkova, O. Kamyshnikov, A. Nikonova, M. Khaitov, Anti-inflammatory effect of fullerene C60 in a mice model of atopic dermatitis, J. Nanobiotechnol. 14 (1) (2016) 1–11.
[62] M. Hiragun, T. Hiragun, I. Oseto, K. Uchida, Y. Yanase, A. Tanaka, T. Okame, S. Ishikawa, S. Mihara, M. Hide, Oral administration of β-carotene or lycopene prevents atopic dermatitis-like dermatitis in HR-1 mice, J. Dermatol. 43 (10) (2016) 1188–1192.